Zeitschrift: Technische Mitteilungen / Schweizerische Post-, Telefon- und Telegrafenbetriebe = Bulletin technique / Entreprise des postes, téléphones et télégraphes suisses = Bollettino tecnico / Azienda delle poste, dei telefoni e dei telegrafi svizzeri

Herausgeber: Schweizerische Post-, Telefon- und Telegrafenbetriebe

Band: 72 (1994)

Heft: 7

Artikel: Optical fiber characterization by simultaneous measurement of the transmitted and the refracted near field

Autor: Gisin, Nicolas / Passy, Rogerio / Perny, Beat

DOI: https://doi.org/10.5169/seals-874722

Optical Fiber Characterization by Simultaneous Measurement of the Transmitted and the Refracted Near Field[1]

Nicolas GISIN and Rogerio PASSY, Geneva, and Beat PERNY, Berne

Zusammenfassung

Beschreibung optischer Fasern durch gleichzeitige Messung des durchgehenden und des refraktierten Nahfeldes

Es wird ein Versuchsaufbau vorgestellt, der es routinemässig erlaubt, für Forschungsaufgaben das durchgehende Nahfeld bei 1300 nm und 1550 nm sowie das refraktierte Nahfeld bei 820 nm gleichzeitig zu messen, und eine neue Methode zur Eichung des Brechungsindexes vorgeschlagen. Die Reproduzierbarkeit bei der Messung geometrischer Parameter liegt bei ±0,1 μm. Messungen des Modenfeldes in Funktion des Polarisationszustandes von vier verschiedenen polarisationserhaltenden Fasern werden vorgestellt.

Résumé

Description de fibres optiques par mesure simultanée du champ proche transmis et réfracté

On présente un dispositif de mesure permettant par un test de routine de mesurer simultanément à des fins de recheche le champ proche transmis à 1300 nm et 1550 nm ainsi que le champ proche réfracté à 820 nm. Une nouvelle méthode d'étalonnage pour l'indice de réfraction est proposée. La reproductibilité de la mesure des paramètres géométriques est de ±0,1 μm. Des mesures du champ modal en fonction de l'état de polarisation de quatre fibres «hi-bi» sont aussi présentées.

Riassunto

Descrizione di fibre ottiche mediante la misurazione simultanea del campo vicino trasmesso e rifratto

Gli autori illustrano la preparazione di un esperimento che consente di misurare regolarmente, per motivi di ricerca, il campo vicino trasmesso e rifratto a 1300 nm e a 1550 nm come pure il campo vicino rifratto a 820 nm. Per la calibratura dell'indice di rifrazione viene proposto un nuovo metodo. La riproducibilità delle misurazioni dei parametri geometrici è di ±0,1 μm. Gli autori terminano il loro articolo presentando le misurazioni del modo campo in funzione dello stato di polarizzazione di quattro diverse fibre «hi-bi».

Summary

Optical Fiber Characterization by Simultaneous Measurement of the Transmitted and the Refracted Near Field

We present an experimental setup which permits, in a routine way for R & D purposes, simultaneous measurement of the transmitted near field at 1300 nm and at 1550 nm and the refracted near field at 820 nm. A new method for the calibration of the refractive index is proposed. The reproducibility of measurements of geometrical parameters is ±0.1 μm. Measurements of the mode field in function of polarization state for four different hi-bi fibers are also presented.

1 Introduction

Fast and accurate optical fiber characterization in one experimental setup with a unique fiber preparation is a need of fiber producers and R & D laboratories. The most important parameters to characterize optical fibers are the mode field, cut-off wavelength, geometry, dispersion, and attenuation. The standardization of the measurement methods by the two main international committees, CCITT [1, 2, 3] and IEC [4, 5], is well established. *Table I* shows important fiber parameters and the corresponding reference (RTM) and alternative (ATM) test methods recommended by these two committees.

One of the most powerful methods to retrieve the most information from a fiber with a single fiber preparation step is the measurement of the transmitted and refracted near field (TNF and RNF). Whereas the first one is recommended by CCITT and IEC as a test method for the mode field, the second one is recommended by both committees for the determination of the geometrical parameters of the fiber.

11 Refractive Index Profile

The refractive index (RI) is not specified by the different standardization committees because the optical transmission properties of the fiber are already determined by the mode field diameter (MFD), the cut-off wavelength, and the chromatic dispersion. However, the knowledge of the RI profile permits one to calculate directly the geometrical parameters and, on a theoretical basis, make an estimation of the transmission properties (e.g. the chromatic dispersion, but not the attenuation or the polarization dispersion, since the latter are determined by local defects along the fiber). The most popular techniques for obtaining the RI profile of optical fibers are the transmitted and refracted near-field methods. Due to the leaky mode problem, we have used the RNF for RI profiling. The weak point of this method in most instruments is the use of the liquid's RI for calibration; however, the accuracy of the RI profile can be significantly improved if both the transmitted and the refracted near field are measured simultaneously. The improved RI difference Δn is obtained by adjusting the value of Δn until

Table I. Recommended test methods for optical fiber characterization

Parameter	RTM	CCITT ATM	IEC
Modefield	Far-field	1. Variable aperture 2. Knife edge 3. Transmitted near-field	1. Transverse offset 2. Transmitted near field 3. Far-field
Cutoff λ_c	Transmitted power	Split-Mandrel	1. Transmitted power 2. Mode field vs. wavelength
Dispersion λ_0, S_0	Phase shift	1. Interferometry 2. Pulse delay	1. Pulse delay 2. Phase shift
Geometry Cladding diameter Mode field conc. error Cladding noncircularity	Transmitted near field	1. Refracted near field 2. Side-view 3. Transmitted near-field imaging	1. Refracted near field 2. Transmitted near field 3. Mechanical diameter measurements
Attenuation coefficient	Cut-back	1. Backscattering 2. Insertion loss	1. Cut-back 2. Insertion loss 3. Backscattering

the MFDs as computed from the TNF and the RNF — by numerical integration of the scalar wave equation — agree within the instrumental uncertainty of 0.1 μm. In this way the RNF calibration problem is recovered by the second, independent TNF measurement.

12 Mode Field

An exact knowledge of the mode field diameter (MFD) of a fiber permits calculation of various propagation characteristics such as source-to-fiber coupling, splice loss [6], microbending loss [7, 8], and dispersion [6, 9, 10].

Serveral techniques have been proposed in the literature to measure the spot size from measurements of the transmitted near or far field [11, 12]; however, for routine measurements a far-field scan is too time-consuming and technically very demanding because of the necessary large-angle scans and the high dynamic range needed. Therefore, the method has been modified to the so-called variable aperture in the far-field (VAFF) method [13, 14]. This method is related to the far field by a simple integration [15], permits very fast routine measurements and is already available on commercial instruments [16, 17]. The disadvantage of these instruments is that they do not permit a determination of the geometrical parameters of the fiber already prepared, such as cladding noncircularity and mode field concentricity error, for instance.

We have implemented the TNF method because the near-field distribution can be measured down to levels approximately 40 dB below the maximum level and the mode field results can then be evaluated with an uncertainty of 1 % or about 0.1 μm [18]. Moreover, this method can be implemented together with the RNF method in a single optical setup.

In the next section we recall the main relations used to compute the RI profile, MFD, and chromatic dispersion from the measured TNF and RNF. The experimental setup is presented in Section 3. Results on circular and noncircular fibers are dicussed in Sections 4 and 5, respectively.

2 Transmitted and Refracted Near Field

The organization of this section follows closely *Figure 1.* A historical overview of the development of the different MFD definitions is given in [19].

A transmitted near-field scan provides directly the light intensity distribution $E^2(r)$ at the outcome of the fiber. However, the MFD actually recommended by CCITT is calculated with the well-known Petermann II equation [1, 8], which relies on the far-field intensity distribution $F^2(p)$:

$$2w_{FF} = 2\sqrt{2}\left[\frac{\int_0^\infty F^2(p)P^3dp}{\int_0^\infty F^2(p)p\,dp}\right]^{1/2} \quad (1)$$

where $p = (2\pi/\lambda)\sin\theta$, θ being the far-field angle and λ the wavelength.

The definition of the Petermann II MFD is very convenient, because it is the relevant parameter which affects splice losses due to misalignments [20], bending loss, and dispersion. Joint losses are inversely proportional to $(2\underline{w}^2)$ [21].

In the approximation of small angles θ, Hotate & Okoshi [12] showed that the near field E(r) and the far field F(p) form a Hankel pair (Fourier-Bessel transform) are

$$F(p) = \int_0^\infty E(r)J_0(rp)r\,dr$$
$$E(r) = \int_0^\infty F(p)J_0(rp)p\,dp \quad (2)$$

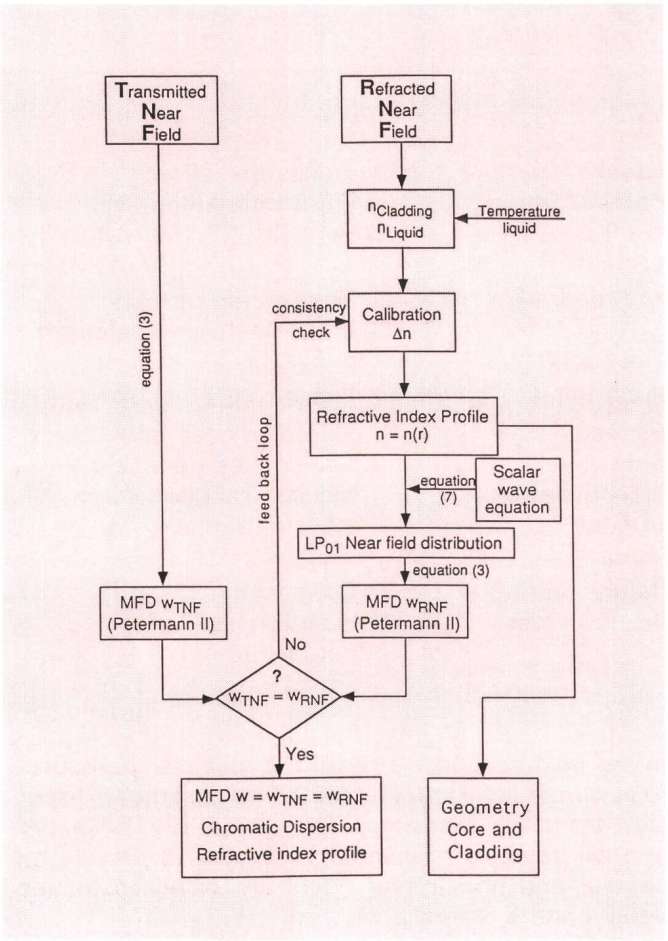

Fig. 1 Relation between experimental data and the derived optical parameters. The consistency check of the refractive index calibration is shown by the feedback loop

where r is the radial distance from the center of the fiber's core in the plane of the fiber's end face and J_0 is the zero-order Bessel function.

Equation (2) permits one to pass from the near field to the far field and reverse. Therefore, the MFD $2w_{FF}$ as recommended by CCITT can be calculated in terms of near field E(r) [21]:

$$2w_{TNF} = 2\sqrt{2}\left[\frac{\int_0^\infty E^2(r)\,r\,dr}{\int_0^\infty \left(\frac{dE(r)}{dr}\right)^2 r\,dr}\right]^{1/2}$$

Since we are measuring $E^2(r)$, we use the following equivalent form:

$$2w_{TNF} = 2\sqrt{2}\left[\frac{\int_0^\infty E^2(r)\,r\,dr}{\frac{1}{4}\int_0^\infty \frac{1}{E^2(r)}\left(\frac{d(E^2)}{dr}\right)^2 r\,dr}\right]^{1/2} \qquad (3)$$

Equation (3) can easily be programmed and is numerically stable. The main practical difficulty is to extend the integration to infinity. In our case with 30 dB dynamics, a pragmatic solution that we have implemented consists first of a numerical integration using the data until above the noise level. The right and left tail of the data (still above the noise level) are then fitted by the exponential of a quadratic polynomial:

$$E^2(r) \approx \exp\{ar^2 + br + c\} \quad for \frac{E^2(r)}{E^2_{max}} \le 0.05 \qquad (4)$$

Finally, using these two fits, the numerical integration can be extended below the noise level. Without these fits a higher dynamics (40 dB) would be needed to obtain the numerical accuracy for the MFD W_{TNF}, between 1 % and 3 %, depending on the fiber profile.

The relation between the RI distribution and the RNF scan is not as direct as between a TNF scan and the light intensity distribution (Fig. 1). However, provided that the RI variation is not too large (a condition easily met for optical fibers) and the profile of the light beam used for the RNF scan is Lambertian [22, 23], it is close to a simple linear relation. Also, the collection optics should have a constant efficiency and the 'blocking disk' should be large enough to block all the leaky modes (see below). This linear relation can be best tested using calibration fibers that are produced specially for this purpose (see Section 4). Once the linear relation is established, the relation between the RI profile and the RNF scan is reduced to the determination of two parameters. These parameters are usually taken as the RI values of the pure silica cladding (or pure silica core in appropriate cases) and of the immersion liquid. The first value is quite stable within a production line, but may vary significantly from one type of fiber to another, $\delta n = 0.0007$ [24]. The second value is more critical, since it depends on the liquid temperature and its purity. In principle these conditions can be controlled, or at least the temperature can be measured independently. But experience has shown that the RI of the immersion liquid is the main cause of error in the RNF technique for RI profiling. Calibration uncertainties up to 10 %, depending on the magnitude of the refractive index difference between the immersion liquid and the cladding, are possible [25, 26]. We shall come back to this calibration problem at the end of the present section and in the next section.

Another potential source of error are the leaky modes. These are the nonguided modes that propagate along the fiber over short distances. If such leaky modes are detected, the calibration overestimates the RI. The leaky modes propagate in the cladding at angles θ_l with respect to the fiber axis smaller than [27]:

$$\tan\theta_l \cong \sqrt{2\frac{\Delta n}{n}} \qquad (5)$$

where Δn is the maximum index difference. Allowance for the refraction at the cladding-liquid interface

shows that the maximum Δn without leaky mode effects is given by

$$\Delta n \leq \frac{n}{2}\left(\frac{n_{min}^2}{n_{liq}^2 \cos^2 \theta_c} - 1\right) \qquad (6)$$

where θ_c is the minimum angle at which rays are detected. For an angle $\theta_c = 14°$ and matched cladding fibers for this formula gives $\Delta n < 0.032$ $n_{min} = 1.457$, and $\Delta n < 0.021$ for $n_{liq} = 1.47$ and 1.58, respectively. For the same angle and liquids, but with a deeply depressed cladding of $n_{min} = 1.45$, the inequalities are $\Delta n < 0.024$ and $\Delta n < 0.014$, respectively. Therefore, we did not expect leaky mode problems for the telecommunication fibers considered in this article; however, deeply depressed fibers may show leaky mode effects. This is in good agreement with our results; in particular, the typical ear-like profile due to leaky modes can be seen on the calibration fiber *(Fig. 4)*. (Note, however, that the level III is wide enough to nevertheless allow the determination of its refractive index.)

All the propagation parameters (except attenuation and polarization mode dispersion) are determined by the distribution of the RI profile of an optical guide. It is possible to numerically integrate the scalar (or vector) field equation and thus compute from the RI profile the propagation constants (i.e. the group velocity in function of wavelength), hence the chromatic dispersion, and the mode field distribution of the fundamental mode (Fig. 1). The same could also be done for all modes, and the theoretical cut-off can also be computed, but we shall not consider these possibilities here.

Since this method of determining the mode field and the chromatic dispersion requires considerable computation, the relation between the data and the computed parameters is not direct; however, some of the computed parameters are not too sensitive to the data [28].

The scalar wave equation for the fundamental mode LP_{01} reads

$$\frac{d^2E(r)}{dr^2} + \frac{dE(r)}{r\,dr} + k^2 n^2(r) E(r) = \beta^2 E(r) \qquad (7)$$

where r, k, n(r), and β denote the radical coordinate, the wave number in vacuum, the refractive index profile, and the propagation constant of the LP_{01} mode, respectively. We use the Numerov integration method [29]. Note that the eigenvalues β are directly related to the propagation constant. One can thus determine the part of the chromatic dispersion due to the waveguide shape by determining the propagation constant for several wavelengths [30]. Once the value of β is determined, (7) can be integrated numerically, thus providing the mode field distribution. The MFD W_{TNF} can be directly deduced using relation (3). For the fundamental mode LP_{01} the computed MFD W_{RNF} (Fig. 1) is not sensitive to the details of the RI profile. It is, however, quite sensitive to the global scale of the RI profile, e.g. to a global enlargement or compression of the RI profile. *Figure 2* shows the sensitivity of the computed MFD W_{RNF} in function of the RI difference Δn between the maxima of the core and the cladding (the shape of the RI profile is kept fixed). Note that the interlaboratory reproducibilities σ_{IL} in the COST 217 Round Robin [31] for the determination of the RI difference Δn varied between $\sigma_{IL} = 0.0004$ and 0.0014, depending on fiber type. Such large deviations could result in differences up to 1 μm for calculated MFD's and 30 nm for zero dispersion.

This leads us to the 'feedback loop' in Figure 1. We take advantage of the fact that both techniques provide a value, W_{TNF} and W_{RNF}, for the MFD to check the calibration of the RI profile independently of the RI of the immersion liquid. This is useful, since it is well known [26, 31] that large errors may occur and that it may be difficult to notice them. The consistency check that we propose is done by adjusting the global scale of the RI profile until the MFD W_{RNF} computed from the RI profile scaled to the appropriate wavelength using Flemming's data [33] agrees with the MFD W_{TNF} measured in the TNF. The Fleming data take into account the material dispersion whose uncertainty is much smaller than our measurement error. In this way we can avoid all the problems with liquid temperature variations, temperature gradients, and liquid pollution; therefore, one may also expect an exact determination of the chromatic dispersion from the simultaneous TNF and RFN scans.

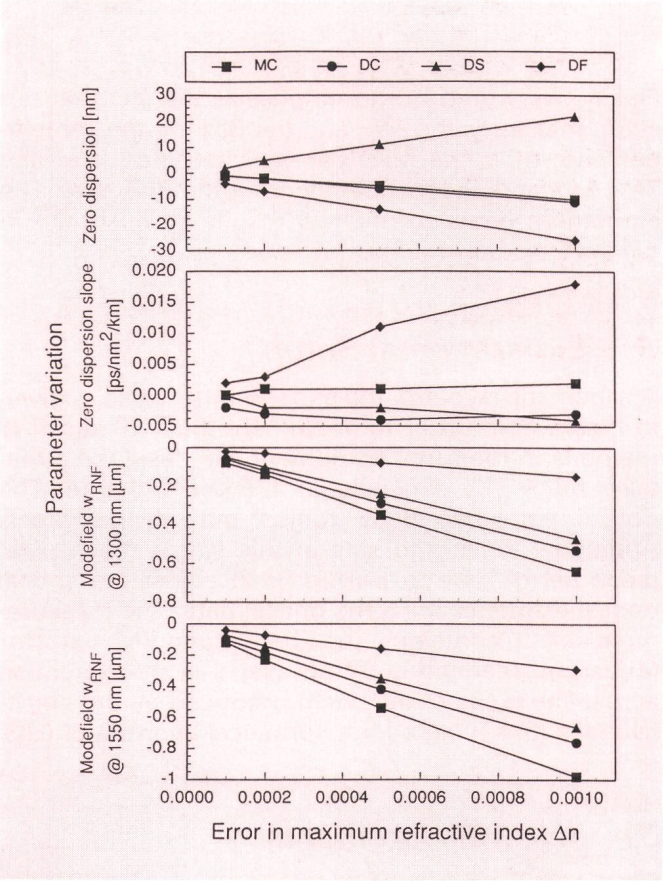

Fig. 2 Variation of optical transmission parameters versus error in maximum refractive index Δn

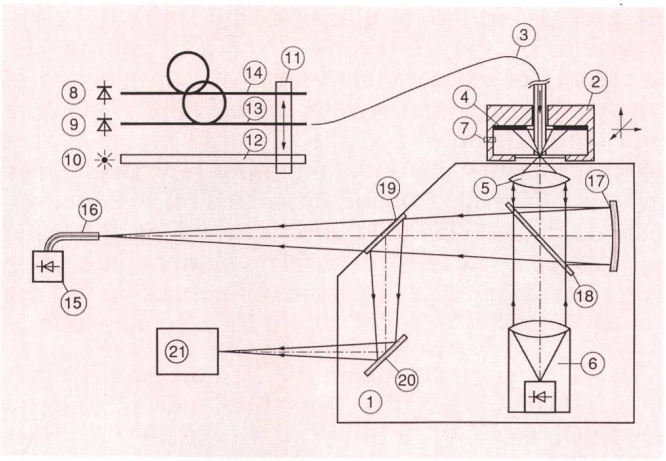

Fig. 3 Schematic layout of the experimental setup

1 Metallic block (115×60×90 nm)
2 Measurement cell
3 Fiber under test
4 Si detector for the RNF
5 Objective lens
6 820-nm collimated laser source for the RNF
7 Temperature sensor
8 1300-nm laser source for the TNF
9 1550-nm laser source for the TNF
10 White light source
11 Movable fiber support
12 White light fiber bundle
13 Fiber pigtails
14 Fiber pigtails
15 InGaAs detector for the TNF
16 Multimode fiber (30-μm core)
17 Parabolic mirror
18 Pellicular beam splitters
19 Pellicular beam splitters
20 Mirror
21 CCD camera

Finally, we would like to emphasize the fact that our setup measures the TNF and the RNF on the same fiber end; thus, the MFD can be computed from the TNF data and, independently, from the RNF data. The agreement between the two results is illustrated in *Figure 5*; see also [24].

3 Experimental Setup

A schematic layout of the experimental setup is given in *Figure 3*. In order to implement the TNF and RNF methods in the same equipment, we designed a metallic block (1); dimensions: 115×60×20 mm. The optical path has been tooled out of this block. Additional holes and slits in this single mechanical piece permit one to position and adjust the critical optical elements along the optical path. The measurement cell (2) containing the fiber (3) and RNF detector (4) can be scanned in 0.1-μm steps in x-y-z direction across the focus of the beam produced by the objective lens (5) having a high numerical aperture of 0.83.

31 RNF Measurements

For the RNF measurements, light emitted by an optically stabilized 820-nm collimated laser (6) focused on the immersed fiber end by an objective (5). This avoids unacceptable cut-offs in the spatial frequency domain. The measurement cell (2) is characterized by the fact that the detector, a large surface silicon detector (4) with an annular shape, is immersed into the liquid, dispensing with any collecting optics, avoiding thus changes in detection efficiency with angular changes [24] and polarization-dependent reflections and refractions. It is identical to the one described previously [34], with two exceptions: 1. The temperature sensor (7) is in contact with the liquid in the cell; this greatly improves the determination of the liquid's temperature and thus its refractive index, which is used for the initial refractive index calibration. 2. Single-mode and multimode fibers can be analyzed in the same cell, whose geometry has been optimized for spatial resolution [22] and for avoiding leaky modes. The portion of the rays refracted out of the side of the fiber is collected by the annular detector (4). The variation in detected signal is proportional to the index changes encountered at the fiber end face during a scan across the focus of the beam. Knowing the liquid index and the pure silica cladding index, a linear interpolation provides the refractive index scale. The index data can be scaled on line to other wavelengths, using Fleming's data [33]. Due to the Lambertian shape of the 820-nm laser beam (6), nonlinearity corrections are not necessary, contrary to the case of a 633-nm HeNe laser beam [35].

Complete fiber geometry measurements are done by recognizing the cladding and core limits in about ten different x, y scans and fitting a circle or ellipse through these points. The whole procedure takes about one minute (after fiber installation).

32 TNF Measurements

Once the fiber is focused and centered for the RNF, the NF analysis can be started after injecting laser radiation of wavelength 1.3 μm (8) or 1.55 μm (9) into the second fiber end. An alignment system (11) allows one to switch in a few seconds from a white-light fiber bundle (12) to one of the two lasers' single-mode pigtails (13 or 14). An InGaAs detector (15) pigtailed to a 30-μm-diameter step index multimode fiber (16) is placed at the focal point of the parabolic mirror (17) to detect the TNF light. This fiber provides a good compromise between the signal-to-noise ratio (as with a single-mode fiber) and the resolution (as with a standard multimode fiber). Moreover, it is easier to align than a pinhole, which would have the same effect. To avoid multiple reflections, only pellicular beam splitters (18, 19) are used. Since the fiber (3) is moved, and not the detector, the spatial meter is given mechanically by the step motors and is independent of the enlargement factor of the near-field image.

Differences in focal length between the three light sources have been determined with a dispersion-flattened fiber which is very sensitive to defocusing (e.g. 200 μm, from 820 nm to 1300 nm). The program automatically adjusts the fiber to the focal position, depending on the selected type of measurement.

The optical centers of the near field and the refracted near field are slightly different. Their exact positions are determined before each measurement.

For both TNF and RNF, a three-dimensional (3D) view of the measured fields and the refractive index profile can be obtained. Contour levels for individually selected levels can be plotted for more complicated geometry determinations (e.g. ring diameter of dispersion-shifted fibers).

33 Fiber Alignment

White light (10) is launched into the second end of the fiber. The last end is viewed on the TV screen (21), which makes it easy to focus and precenter the core. This manual adjustment is then followed by an automatic adjustment procedure, which consists of the focusing of the fiber for the transmitted or refracted near field by maximizing the Fourier transform spectra and of the determination of the optical center by minimizing the left-right differences.

A bar-graph system connected with the near-field (15) and refracted near-field detector (4) shows the amount of launched light from one of the three sources (6, 8 or 9).

Similarly, the axis of high wire-fringent fibers can be located with the TV system. If a polarizer is then introduced in front of the TNF detector (15), one can measure the mode field for different polarization states.

4 Results and Calibration

41 Refractive Index Linearity

The linearity of the refractive index calibration was checked by measuring a multistep fiber calibrated by the National Physical Laboratory in the United Kingdom (NPL). This fiber provides three calibrated steps, where the difference in relation to the pure silica is shown in Figure 4. The certified values were measured by the NPL using an interferometric technique. The same fiber has been used by the COST 217 group for the comparison of the methods used by the various laboratories [31]. Our measured values are displayed in *Table II.* We can observe that the maximum index difference between the certified values and our values does not exceed 0.0003. The refractive index resolution using cis-decahydronaphtalen ($n \approx 1.478$) as calibration liquid is 0.0001. Table II shows also the values obtained with a He-Ne laser having a Gaussian beam [35].

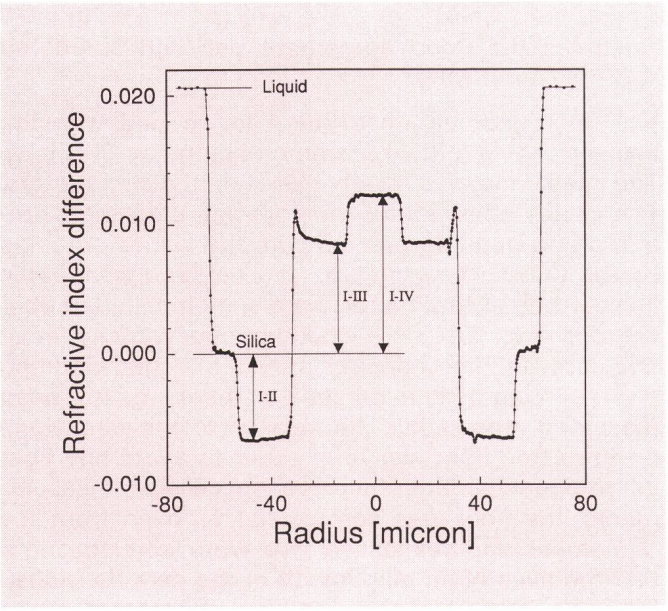

Fig. 4 Measured refractive index profile of a calibration fiber delivered by the National Physical Laboratory

Table II. Refractive index differences for a special calibration fiber obtained with our instrument, compared to the values certified by the national physical laboratory

	Refractive index difference × 10^{-3}		
	Level I—II	Level I—III	Level I—IV
National Physical Laboratory	6.7	8.1	11.7
Our instrument[1]	6.7	8.4	11.9
Gauss analysis	7.9	10.3	14.0

[1] Obtained with 820-nm laser source having a Lambertian shape.
[2] Obtained with a Gaussian beam of a HeNe laser when no nonlinearity correction is applied [34].

42 Spatial Resolution

To evaluate the spatial resolution, a dispersion-flattened fiber was measured. This fiber has a particular index profile with a very thin ring around the core (see Fig. 5). The resolution was thus tested by measuring the maximum index difference between the core and the thin depressed ring of this fiber. The difference between the value measured and the value reported in [31] was smaller than 0.0004. The spatial resolution obtained with this system is about 0.1 to 0.2 μm for both measurements.

43 Mode Field Diameter and Geometrical Parameters

Six fibers used by the COST 217 group [31] were measured. Some measurements were repeated after a time interval of nine months. Our results are reported in *Table III.* They include possible inhomogeneity within the samples. The maximum Δn remains for all profile structures within the variations of the COST 217 interlaboratory reproducibility.

For the MFD measurements the accurarcy of the equipment was tested using the same six fibers

Table III. Optical fiber parameters obtained in a measurement campaign of COST 217 [31] compared with the values measured with our instrument

	Pure silica	Matched cladding	Depressed cladding	Dispersion shifted (ring)	Dispersion shifted (no ring)	Dispersion flattened
			Maximum refractive index difference $\times 10^{-3}$			
COST 217	5.3 ± 0.9	5.4 ± 0.4	6.4 ± 0.7	11.7 ± 0.8	10.7 ± 0.7	18.6 ± 1.4
Our instrument	5.55 ± 0.15	5.3 ± 0.0	6.4	11.5 ± 0.1	10.55 ± 0.15	18.2 ± 0.2
			Mode field diameter @ 1300 nm [μm]			
COST 217	9.61 ± 0.24	9.43 ± 0.29	9.02 ± 0.23	6.77 ± 0.49	6.40 ± 0.65	5.99 ± 0.16
Our instrument	9.65 ± 0.15	9.6 ± 0.2	9.2	6.35 ± 0.55	6.25 ± 0.05	6.15 ± 0.05
			Mode field diameter @ 1550 nm [μm]			
COST 217	10.95 ± 0.41	10.82 ± 0.36	10.17 ± 0.35	8.68 ± 0.71	7.78 ± 0.92	6.99 ± 0.51
Our instrument	10.85 ± 0.05	10.7 ± 0.1	10.3	8.3 ± 0.1	7.2 ± 0.4	7.0
			Core diameter [μm]			
COST 217	8.83 ± 0.14	7.63 ± 0.15	8.22 ± 0.29	3.92 ± 0.31	4.28 ± 0.14	5.58 ± 0.18
Our instrument	9.0 ± 0.0	7.55 ± 0.15	8.0	4.15 ± 0.05	4.15 ± 0.05	5.4
			Cladding diameter [μm]			
COST 217	125.4 ± 0.3	125.2 ± 0.5	125.4 ± 0.4	124.6 ± 0.5	126.33 ± 0.3	126.1 ± 0.4
Our instrument	125.6	125.15 ± 0.25	125.7	125.2 ± 0.2	126.95 ± 0.05	125.9 ± 0.2

Some of our measurements were repeated after nine months. In that case the average values with their deviation are shown. Errors reported for the COST 217 measurements are the interlaboratory reproducibilities. Refractive index differences are for λ = 632.8 nm. For an interlaboratory evaluation of theoretical modeling see [32]

reported in [31] and making a comparison between our values and the average value given by the COST 217 group. The values shown in Table III are calculated using the Petermann II definition, taking the measured data above 5 % of maximum level and the Gaussian fit of the tails below these 5 %. This procedure has increased the reproducibility and made the measurements less sensitive to the noise. The reproducibility using this method was around 0.05 μm on the same fiber end and 0.1 μm on different fiber ends. An example is shown in Figure 5. The general agreement is within the interlaboratory reproducibility (with the noticeable exception of the MFD at 1.3 μm for the dispersion-shifted fiber with a ring whose first measured value was too low). Figure 5 illustrates the good agreement between computed and measured MFD.

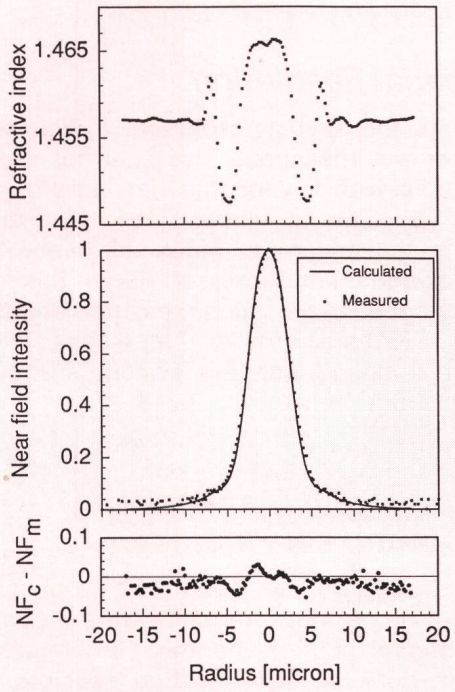

Fig. 5 Measured refractive index profile, the corresponding computed and measured near field, and their difference for a dispersion-flattened fiber

The fiber geometry has been determined with the RNF according to the recommendations by CCITT [1]. The spatial meter is simply based on the step motors. The values obtained for the core and cladding diameter are in good agreement with the values obtained by the COST 217 group, as can be seen from Table III, with one exception for the dispersion-shifted fiber without ring. For core-cladding concentricity error and core-cladding noncircularity, a matched cladding and a ring-dispersion-shifted fiber have been measured repeatedly. The measurements were done on the same fiber cleave in order to avoid any fiber inhomogeneity, but, between successive measurements, the fiber was completely removed from the equipment and reinstalled. We were able to check that the axes of an elliptical fit of the data do indeed follow a rotation of the fiber and that the standard deviations of all the measured core and cladding diameters are close to 0.1 μm, which is the resolution of the setup. The results are summarized in *Table IV.*

Table IV. Reproducibility of geometrical parameters of two different fiber types (MC = Matched Cladding Dispersion Normal, DS = Dispersion Shifted With Ring)

	Circular fit						
Fiber type	Core diameter [μm]		Cladding diameter [μm]		Concentricity error [μm]	Noncircularity [%]	
MC	8.33 ± 0.09		124.94 ± 0.06		0.11 ± 0.04		
DS	4.46 ± 0.03		125.68 ± 0.07		0.23 ± 0.09		
	Elliptic fit						
	Big axis	Small axis	Big axis	Small axis		Core	Cladding
MC	8.46 ± 0.13	8.19 ± 0.08	125.7 ± 0.1	124.6 ± 0.1	0.09 ± 0.04	3.2 ± 0.2	0.6 ± 0.2
DS	4.54 ± 0.11	4.38 ± 0.1	126.0 ± 0.1	125.4 ± 0.2	0.23 ± 0.09	3.6 ± 1.7	0.5 ± 0.2

The values are obtained from seven measurements without new cleaving but new positioning and approx. 20° turning of the fiber around the vertical axis for each measurement.

These satisfactory results were due to the accurate alignments of the x-y axis perpendicular to each other. Indeed, for a misalignment $\pm\delta\theta$ with respect to the exact 90° angle, a perfectly circular fiber would appear as an ellipse of noncircularity p:

$$p = \frac{2\sin\delta\theta}{1+\cos\delta\theta}$$

For a 1° error $\delta\theta$, the apparent noncircularity would already be of 1.75 %. However, the factory specifications of the motors we used (i.e. $5 \cdot 10^{-5}$ rad) guarantee an apparent noncircularity of 0.05 %.

5 MFD versus Polarization

Using the TV image and x-y RNF scans, one can locate the axis of hi-bi fibers. After switching the 1.3- or 1.55-μm laser source, the state of polarization can be adjusted by introducing a polarizer in front of the TNF detector. The lo-bi fiber laser's pigtail is then moved until the linear polarized light emerging from the fiber is aligned on the polarizer. The latter is then removed so as not to alter the measurement resolution. With this procedure, the MFD of each fiber was measured 20 times for both polarization states, and the average and standard deviations were computed. The obtained results are summarized in *Table V.* It is clearly visible that the MFD of hi-bi fiber are independent of polarization, which confirms the results from Villuendas [36].

6 Conclusion

An experimental setup which permits measurement of TNF and RNF on the same fiber end with only one fiber preparation has been presented. The instrument

Table V. Mode field diameter for different polarization states

Fiber	Birefringence axis	Polarization axis	Mode field [μm] @ 1300 nm	Mode field [μm] @ 1550 nm
	X	X	8.98 ± 0.02	9.81 ± 0.07
PANDA	X	Y	8.98 ± 0.03	9.80 ± 0.03
	Y	X	9.43 ± 0.03	10.32 ± 0.02
	Y	Y	9.46 ± 0.03	10.39 ± 0.02
	X	X	6.27 ± 0.03	7.10 ± 0.03
YORK	X	Y	6.24 ± 0.03	7.13 ± 0.03
	Y	X	7.22 ± 0.07	7.91 ± 0.04
	Y	Y	7.25 ± 0.03	7.95 ± 0.05
	X	X	7.90 ± 0.03	8.72 ± 0.02
AT & T	X	Y	8.02 ± 0.03	8.71 ± 0.03
	Y	X	7.81 ± 0.02	8.25 ± 0.03
	Y	Y	7.84 ± 0.04	8.26 ± 0.03
	X	X	11.79 ± 0.12	12.71 ± 0.18
CABLOPTIC	X	Y	11.84 ± 0.12	12.51 ± 0.29
	Y	X	8.01 ± 0.10	8.50 ± 0.19
	Y	Y	7.95 ± 0.11	8.36 ± 0.28

is well suited for R & D purposes[2]. The advantages of having simultaneous access to both sets of data have been discussed, with special emphasis on RI profile calibration and reliability of the results. The resolution and the accuracy have been tested by comparing the results obtained with our setup with those obtained during the interlaboratory measurement campaign organized by the COST 217 group and with the NPL-certified calibration fiber. From this we estimate the uncertainty to be $\Delta n = \pm 0.0002$. Geometrical parameters can be determined with an uncertainty of 0.1 μm, including the core-cladding concentricity and elliptical fits for the core and the cladding. Finally, the results show that our setup can also be used to measure the TNF and RNF of hi-bi fibers.

Acknowledgment

The authors gratefully acknowledge the financial support of the Swiss Office fédéral de l'éducation et de la science within the frame of COST 217. The authors also thank Dr. J.-P. Pellaux from Orbisphere Laboratory and Dr. H. R. Haller from the Swiss PTT for stimulating discussions. The technical support from P. Stamp is greatly appreciated. The authors would also like to thank Dr. K. Raine from the National Physical Laboratory for critical reading of the manuscript.

Bibliography

[1] CCITT G.650, Definition and test methods for the relevant parameters of single-mode fibers, 1992.

[2] CCITT G.652, Characteristics of a single-mode optical fiber cable, 1992.

[3] CCITT G.653, Characteristics of a dispersion-shifted single-mode optical fiber cable, 1992.

[4] IEC 793/1 International Standard, Optical fibers, Part 1: Generic specifications, 1991.

[5] IEC 793/2 International Standard, Optical fibers, Part 2: Product specifications, 1992.

[6] *Sharma E. K.* and *Tewari R.* Accurate estimation of single-mode fiber characteristics from near-field measurement. Electron. Lett., vol. 20, 805, 1984.

[7] *Petermann K.* Fundamental mode microbending loss in graded index and W-fibers. Opt. Quantum Electron., vol. 9, pp. 167–175, 1977.

[8] *Sarkar S., Kuman A., Goyal I. C., Charma E. K.* and *Tewani R.* On microbending-loss calculations in single-mode fibers with arbitrary index profiles. Opt. Commun., vol. 53, pp. 91–94, 1985.

[9] *Petermann K.* Constraints for fundamental-mode spot size for broadband dispersion-compensated single-mode fibers. Electron. Lett., vol. 19, pp. 712–714, 1983.

[10] *Sansonetti P.* Modal dispersion in single-mode fibers: Simple approximation issued from mode spectral behaviour. Electron. Lett., vol. 18, pp. 641–648, 1982.

[11] *Anderson W. T.* Spot size measurements for single-mode fibers: A comparison of four techniques. J. Lightwave Technol., vol. 1, pp. 20–26, 1983.

[12] *Hotate K.* and *Okoshi T.* Measurement of refractive index profile and transmission characteristics of a single-mode optical fiber from its exit-radiation pattern. Appl. Opt., vol. 18, no. 19, p. 3265, 1979.

[13] *Dick J. M., Modavis R. A., Racki J. G.* and *Westwig R. A.* Automated mode radii measurement using the variable aperture method in the far-field. Presented at the Technical Digest Conference on Optical Fiber Communication (Atlanta, GA), 1986.

[14] *Saravanos C.* and *Lowe R. S.* New approach for determining non-Gaussian mode fields of single-mode fibers from measurements in the far field. Electron Lett., vol. 21, no. 20, p. 898, 1985.

[15] *Anderson W. T., Shah V., Curtis L., Johnson A. J., Kilmer J. P.* and *Sansonetti P.* Mode field diameter measurements for single-mode fibers with non-Gaussian profiles. J. Lightwave Technol., vol. 5, pp. 211–217, 1987.

[16] Photon Kinetics, Inc., 4900 S.W. Griffith Drive, Beaverton, OR 97005, USA. Model 2500 Analysis System.

[17] York Technology Ltd., York House, School Lane, Chandler's Ford, Hampshire SO5 3DG. U.K. Refractive Index Profiler S14.

[18] *Neumann E. G.* Single-mode fibers. Springer Ser. Optical Sci., vol. 57, 1988.

[19] *Artiglia M., Coppa G., Di Vita P., Polenza M.* and *Sharma A.* Mode field diameter measurements in single-mode optical fibers. J. Lightwave Technol., vol. 7, no. 8, p. 1139, 1989.

[20] *Anderson W. T.* Consistency of measurement methods for the mode field diameter in a single-mode fiber. J. Lightwave Technol., vol. LT-2, no. 2, p. 191, 1984.

[21] *Pask C.* Physical interpretation of Petermann's strange spot size for single-mode fibers. Electron. Lett., vol. 20, p. 144, 1984.

[22] *Stewart W. J.* A new technique for measuring the refractive index profile of optical fibres. Technical Digest 1006 (IECE, Tokyo, 1977), pp. 395–398.

[23] *White K. I.* Practical application of the refracted near-field technique for the measurement of optical fiber refractive index profile. Opt. Quantum Electron., vol. 11, p. 185, 1979.

[24] *Raine K. W., Baines J. G. N.* and *King R. J.* Comparison of refractive index measurements of optical fibres by three methods. IEE Proc., vol. 135, pt. J., no. 3, pp. 190–195,1988.

[25] *Raine K. W., Baines J. G. N.* and *Putland D. E.* Refractive index profiling: State of the art. J. Lightwave Technol., vol. 7, no. 8, p. 1162, 1991.

[26] *Hutjens M.* Round robin results on fiber refractive index differences measured by the refracted near-field method. J. Opt. Commun., vol. 9, p. 92, 1988.

[27] *Marcuse D.* and *Presby H. M.* Index profile measurements of fibers and their evaluation. Proc. IEEE, vol. 68, p. 666, 1980. See also *Mar-*

[2] The Group of Applied Physics of the University of Geneva can produce this instrument upon request: Fax +4122 781 0980

cuse D. Principles of Optical fiber measurements. New York: Academic Press, 1981.
[28] *Pelayo J.* In COST 217 Final Report, Bruxelles, 1993 (in press).
[29] *Davies R. W., Davidson D.* and *Singh M. P.* Single-mode optical fiber with arbitrary RI profile: Propagation solution by the Numerov method. J. Lightwave Technol, vol. 3, pp. 619–627, 1985.
[30] *Thévenaz L.* Effets et mesure de la dispersion dans les guides d'ondes optiques. Ph.D. thesis, University of Geneva, 1988.
[31] COST 217 Group, Interlaboratory measurement campaign on single-mode fibers. IEE Proc., pt. J., vol. 136, pp. 307–314, 1989.
[32] COST 217 Group, Interlaboratory evaluation of theoretical modelling techniques for single-mode optical fibers. IEE Proc., pt. J, vol. 139, pp. 353–356, 1992.
[33] *Fleming J. W.* Material and mode dispersion in GeO-B_2O_3-SiO_2 glasses. J. Am. Ceram. Soc., vol. 59, pp. 503–507, 1976.
[34] *Pellaux J.-P., Witschi A.* and *Bischofberger T.* Messgerät zum Bestimmen des Brechungsindexprofils einer Glasfaser. Bern, Techn. Mitt. PTT, Vol. 63 (1985), Nr. 4, S. 138–151.
[35] *Gisin N.* and *Raine K. W.* Correcting refracted near-field refractive index profile measurements for Gaussian intensity distributions. Opt. Commun., vol. 83, no. 56, p. 295, 1991.
[36] *Villuendas F., Calvo F.* and *Marqués J. R.* Measurement of mode field radians in axially nonsymmetrical single-mode fibers with arbitrary power distribution. Opt. Lett., vol. 12, p. 941, 1987.

Nicolas Gisin was born in Geneva, Switzerland, in 1952. He received his Ph.D. degree in physics from the University of Geneva in 1981 for his dissertation in quantum and statistical physics. In 1985, after a postdoctoral position at the University of Rochester, NY, he joined the Alphatronix company. Since 1988 he is head of the optics section of the Group of Applied Physics at the University of Geneva. His research work ranges from quantum optics to fibers and integrated optics.

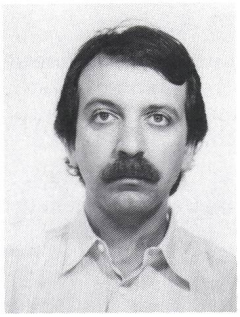

Rogerio Passy was born in Rio de Janeiro, Brazil, in 1963. He received the B.E. degree in electrical engineering and the M.Sc. in physics from Pontificia Universidade Catolica (PUC) do Rio de Janeiro and the Ph.D. degree from University of Geneva, Switzerland, in 1985, 1991 and 1993 respectively. From 1983 to 1990 he worked in the Physics Department of PUC where his work involved optical fiber metrology, underwater optical communication systems and optical sensors. In 1991 he joined the Group of Applied Physics at the University of Geneva where he worked on the optical fibre characterisation including refractive index profile and polarization mode dispersion. He is currently working on optical frequency domain reflectometry.

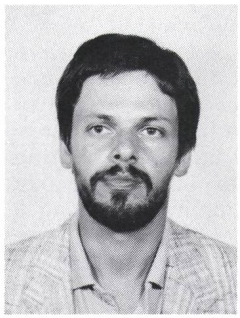

Beat Perny was born in Switzerland in 1958. Her received the Ph.D. degree in atomic and nuclear physics from the University of Freiburg, Switzerland, in 1987. From 1987 to 1990 he obtained a postdoctoral position at the University of Berne, Switzerland, where he worked in the field of secondary ion mass spectrometry and trace element analysis of quartz glasses. In 1990 he joined the Optical Fibre Cable Group of the Research and Development Department of Swiss Telecom PTT. Since 1992 he is head of the group where he is currently engaged in optical transmission aspects of optical fibres and cables.